Modelling of Nickel Laterite Smelting to Ferronickel

Douglas R Swinbourne
School of Civil, Environmental and Chemical Engineering,
RMIT University, 124 Latrobe Street, Melbourne 3000, Australia.

Keywords: nickel laterite smelting, ferronickel

Most nickel is produced as the metal, but about a third of the world's new nickel is ferronickel. World annual production of ferronickel is around 250,000 tonnes, with the two largest producers being BHP Billiton and Société Le Nickel (Cartman, 2010). Most of the world's accessible nickel reserves are oxidic ores called "laterite" (Sudol, 2005), and are the result of chemical weathering and supergene enrichment of mafic/ultramafic rocks. They vary greatly in depth, nickel grade and mineralogy (Dalvi *et al*., 2004). The lower layers are called "saprolite" and have nickel contents from 1.8 to 3 wt-%, relatively low iron contents but high magnesia and silica contents and are suited to pyrometallurgical processing (Cartman, 2010).

Laterite is mined by open cut methods, upgraded by screening to remove low-nickel bedrock, then crushed (Figure 1a). It contains about 35 wt-% free water so is dried in a rotary kiln, with the product still containing approximately 10 - 13 wt-% water. Most of this water is chemically bound within such minerals as garnierite $(Mg,Ni)_3Si_2O_5(OH)_4$ so 700 to 900^oC is needed to remove it. The dried material, with some added coal, passes to rotary kilns where a flame heats the material. The coal volatiles and some of the fixed carbon partially reduce the ore. The remaining fixed carbon acts as the reductant in the following smelting step. Hot calcine is fed to an electric furnace (Figure 1b) where the remaining Fe_3O_4 is reduced to FeO and the NiO and CoO, together with part of the FeO, are reduced to molten ferronickel. The gangue oxides form slag. Finally, the molten ferronickel is refined to remove phosphorus and sulphur and, if necessary, to adjust the carbon and silicon contents to meet market specifications Crundwell *et al*. (2011). The flowsheet described above is commonly referred to as the "RKEF process" (Walker *et al*., 2009) due to its use of rotary kilns (RK) and electric furnaces (EF). Typical industrial data was given by Warner *et al.* (2006) and part of this is shown below for several smelters.

Table 1 – Typical industrial data from Warner et al. (2006)

	Laterite feed		Alloy Ni grade	Slag/alloy mass ratio	Furnace recoveries		
	Fe/Ni	SiO_2/MgO	wt% Ni		Ni %	Co %	Fe %
1. Falcondo	10.5	1.6	38.5	27.8	90.2	76.3	13.4
2. Codemin	11.7	1.6	28	19.2	91.8	58.7	19.8
3. Cerro Matoso	7.0	2.8	35	13.5	92.8	65.6	24.3
4. Loma de Niquel	11.5	1.3	22.5	17.2	92.2	56.9	27.1
5. Doniambo	4.8	1.75	25	10	94.9	71.1	54.9
6. Pomalaa	6.1	1.6	19	10.9	95.1	69.8	59.1
7. Pamco	6.1	1.6	18.5	8.1	97.0	75.4	65.0

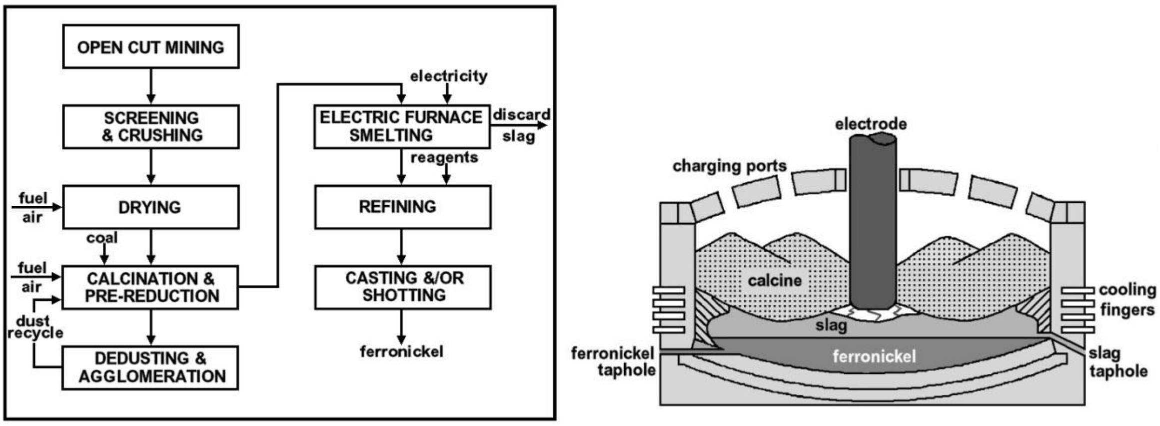

(a) (b)

Figure 1: (a) Flowsheet of ferronickel production from nickel laterite, (b) schematic of electric furnace for smelting of laterite

The oxides in the feed are NiO, FeO, SiO_2 and MgO and the reductant is carbon. The Ellingham Diagram (as shown in Figure 2) shows that at 1500 – 1600°C, under standard state conditions, there is a thermodynamic driving force for the reduction of NiO and FeO by carbon, but that SiO_2 and MgO are too stable to be reduced. Preferential reduction of NiO should be possible. However, NiO is not present at unit activity but is dissolved in slag at low activity. The lines representing the equilibrium oxygen potential of the $Ni/O_2(g)/NiO$ reaction at low NiO activities are also shown. It is now apparent that FeO reduction to iron is favoured when nickel recovery is high. The recovery of nickel will increase as the iron content of the alloy increases and the FeO content of the slag will decrease. However, nickel recovery also depends on the masses of ferronickel and slag produced and the slag mass is always much greater than the ferronickel mass. Solar *et al*. (2008) reported that the mass ratio of slag/ferronickel ranges from approximately 10 to 30 so typical nickel recoveries vary from 90 - 95%. Silicon will also be present in ferronickel at very low activity so a little silica reduction to silicon is expected at the higher extents of reduction. The reduction reactions are strongly endothermic so the required energy input will be large, being typically about 500 kWh/tonne of calcine (Warner *et al*., 2006).

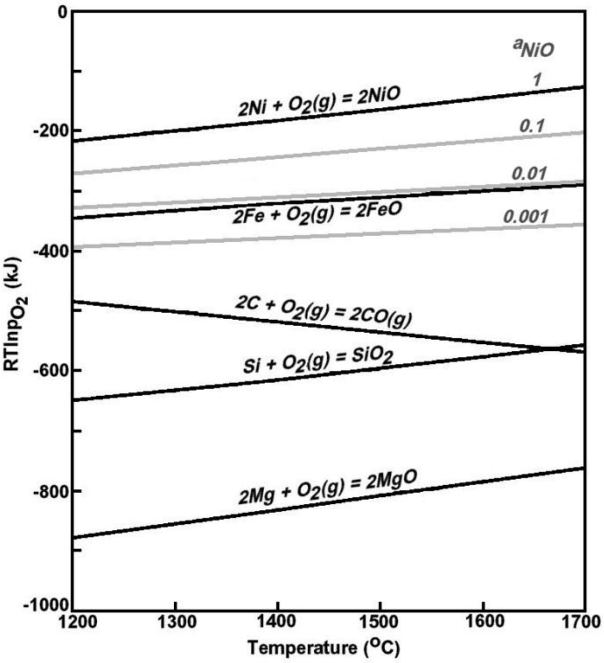

Figure 2: Ellingham diagram for different activity of NiO, FeO, CO, SiO_2 and MgO

The nickel grade of the ferronickel is a function of customer preferences (Solar *et al.*, 2008) and ranges from 17 wt-% to almost 40 wt-% Ni. They showed that the extent of iron reduction is the best indicator of reducing conditions. Ferronickels from high iron reduction smelters contain significant amounts of carbon, silicon and chromium. Liquidus temperatures range from 1450-1460^{o}C for low carbon alloys to 1250 - 1350^{o}C for high carbon alloys. However, the minimum furnace temperature is set by the slag because it typically has a liquidus temperature above 1550^{o}C. In fact a ferronickel furnace is mainly a producer of slag, which comprises over 90% of the furnace output. Modification of the slag composition through the addition of fluxes would require large amounts of flux and so is rarely economic (Utigard, 1994). It follows that the properties of the slag are determined by the SiO_2/MgO ratio of the laterite ore and the concentration of unreduced FeO.

Typical calcine feeds were taken to contain 2 wt-% total Ni, have Fe/Ni (wt-%/wt-%) ratios of 5 and 10 and have a SiO_2/MgO (wt-%/wt-%) ratio of 1.8. Nickel metallisation was taken as 20% and iron oxides were assumed to comprise 40% Fe^{3+} and 60% Fe^{2+} based on the data of Daenuwy and Dalvi (1997). The activity coefficients of all gas species were taken as unity. The activities of iron and nickel in ferronickel alloys were determined by Conard *et al.* (1978) and showed that the activity coefficient of iron is close to unity and that of nickel is 0.65. The activity coefficients of carbon and silicon in molten ferronickel were estimated using the dilute solution model described by Sigworth and Elliott (1974). A representative activity coefficient of carbon was determined to be 1.3 and that of silicon 0.003. Kojima *et al.* (1969) determined the activity of FeO in FeO-MgO-SiO_2 slags at 1600^{o}C. A value of unity was taken to be a satisfactory representation for typical ferronickel slags. The activity coefficient of Fe_3O_4 was taken as unity because it would not be present in the final slag. Experimental activity data for SiO_2 in FeO-SiO_2-MgO slags could not be found so FactSage 6.3.1 software using the FToxid solution database for liquid slag and FSstel solution database for the liquid iron was used to calculate values. A value of unity was also taken to be a satisfactory representation of the activity coefficient of SiO_2(cr) for typical ferronickel slags. The activity coefficient of NiO(s) in FeO_x-MgO-SiO_2 slags at 1500 ^{o}C was determined Henao *et al*. (2001) and an average value for the activity coefficient of NiO(s) of 3.5, independent of the FeO_x content of the slag, was reported. At 1550 - 1600^{o}C the activity coefficient of NiO was taken as 3. The appropriate temperature for modelling was taken to be 1550^{o}C.

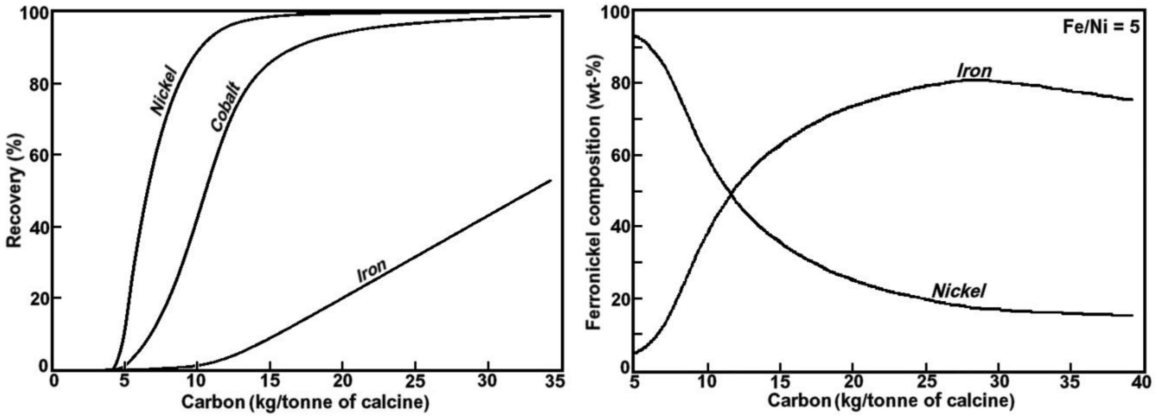

(a) (b)

Figure 3: (a) The recovery of Ni, Co and Fe with carbon (Fe/Ni = 10); (b) the variation of ferronickel composition with carbon (Fe/Ni = 5)

The recoveries of nickel, cobalt and iron are shown in Figure 3(a) for the feed having an Fe/Ni ratio of 10. The recovery of nickel is close to 100% at 20 kg/tonne of carbon, with the cobalt recovery being about 90%. Iron recovery increases almost linearly with the quantity of carbon in calcine. The composition of the ferronickel is shown in Figure 3(b) for a calcine with Fe/Ni = 5. Alloys containing 35 - 40 wt-% Ni require about 10 kg of carbon per tonne of calcine i.e. 1 wt-% carbon in calcine. Alloys containing 17 - 20 wt-% Ni require about 25 kg per tonne of calcine i.e. about 2.5 wt-% carbon in calcine. These carbon contents are in good agreement with those used in practice (Crundwell *et al.*, 2011).

The carbon and silicon contents of ferronickel are given in Figure 4(a), together with the cobalt content, for the calcine having an Fe/Ni ratio of 5. The cobalt concentration quickly reaches a maximum, then decreases as more iron is reduced into the alloy. There is a steep increase in both silicon and carbon contents at high levels of carbon in calcine. For the calcine having an Fe/Ni ratio of 10 the carbon and silicon contents are negligible. These qualitative trends are consistent with published industrial data (Warner *et al.*, 2006). The smelting of calcines with low Fe/Ni ratios results in significant carbon and silicon contents in the ferronickel because when low grade alloys are produced the FeO content of the slag is much lower than when calcines with high Fe/Ni ratios are smelted. The oxygen partial pressure in the system is a function of the concentration of FeO so the oxygen partial pressure is much lower when low Fe/Ni calcines are smelted to low nickel alloys.

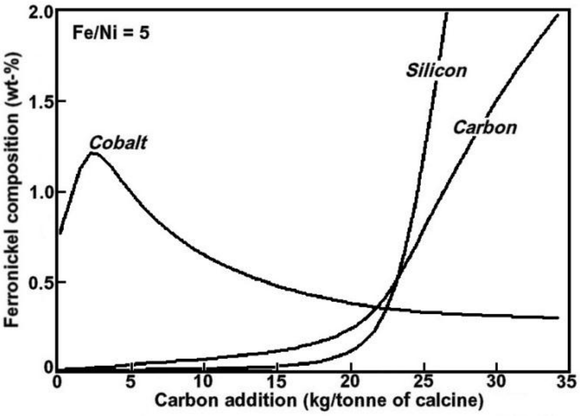

Figure 4: Predicted ferronickel composition, Co, Si and C (Fe/Ni = 5)

Comparison of the model predictions with industrial data is not possible on the basis of the amount of carbon in calcine, because this figure is rarely reported. Solar *et al.* (2008) used the iron recovery in the ferronickel as a measure of the extent of reduction, and this permits useful comparisons to be made. The numerical key for the smelters is given on the table of industrial data (Table 1). The relationship between nickel grade and iron recovery (Figure 5(a)) is shown and the agreement between the model predictions and the industrial data is seen to be excellent. The predicted carbon content of ferronickels was compared to plant data as shown in Figure 5(b). That for the low iron reduction smelters is in acceptable agreement with the predictions, but that for the high iron recovery smelters is not. This discrepancy has also been found by others using different computational thermodynamics software.

No explanation for this discrepancy can be offered. Whatever the cause, it is common to both carbon and silicon, and is unlikely to be thermodynamic in origin because both concentrations are little affected by the extent of iron reduction i.e. the oxygen partial pressure in the furnace.

Overall, the modelling of the electric furnace smelting of nickel laterite calcines has provided useful insights into the nature of the process, especially the way in which the Fe/Ni ratio of laterite and the target nickel grade of the ferronickel affect process performance.

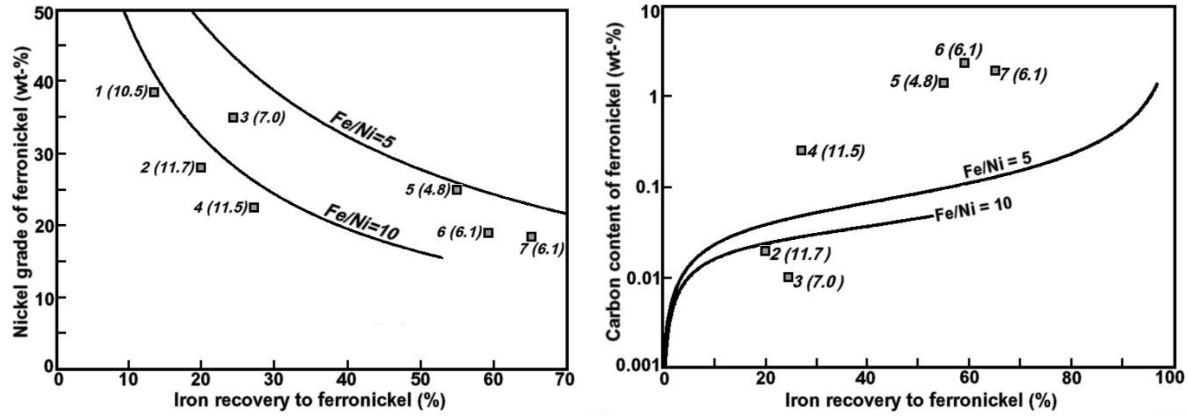

Figure 5: Comparison of the model's results with industrial data in Table 1: (a) nickel grade vs iron recovery, (b) carbon content vs iron recovery

References

Cartman, R. 2010. An overview of the future production and demand of ferronickel, 2^{nd} Euro Nickel Conference, (IMM Informa Australia), http://www.hatch.com.au/Mining_Metals/Iron_Steel/Articles/documents/Future_supply_demand_ferronickel.pdf (accessed on 20 September 2013).

Conard, B. R., McAneney, T. B. and Sridhar, R. 1978. Thermodynamics of iron-nickel alloys by mass spectrometry, *Met. Trans. B*, **9B**, 463-468.

Crundwell, F. K., Moats, M. S., Ramachandran, V., Robinson T. G. and Davenport, W. G. 2011. Extractive metallurgy of nickel, cobalt and platinum-group metals, 67-84, Oxford, Elsevier.

Daenuwy, A. and Dalvi, A. D. 1997. Development of reduction kiln design and operation at PT INCO (Indonesia). in Proc. Nickel-Cobalt 97 International Symposium, (eds. C. Diaz, I. Holubec and C.G. Tan), 93-113, Metallurgical Society of CIM.

Henao, H. M., Hino, M. and Itagaki, K. 2001. Distribution of Ni, Cr, Mn, Co and Cu between Fe-Ni alloy and FeO_x-MgO-SiO_2 base slags, *Materials Transactions of Japan Institute of Metals*, **42**, (9), 1959-1966.

Kojima, V. Y., Inoue, M. and Sano, K. 1969. Die aktiviität des eisenoxyds in FeO–MgO–SiO_2–schlacken bei 1600°C, *Arch. Eisenhuttenwes.*, **40**, 37–40.

Sigworth, G. K. and Elliott, J. F. 1974. The thermodynamics of dilute iron alloys, *Metal Science*, **8**, 298-310.

Solar, M. Y., Candy, I. and Wasmund, B. 2008. Selection of optimum grade for smelting nickel laterites, CIM Bulletin, **11,** (1107), 1-8.

Sudol, S. 2005. The thunder from down under, Canadian Mining Journal, http://www.canadianminingjournal.com/issues/toc.aspx?edition=8/1/2005 (accessed on 15 September, 2013).

Utigard, T.1994. An analysis of slag stratification in nickel laterite smelting furnaces due to composition and temperature gradients, Metall. Trans. B, **25B**, 491-496.

Walker, C., Kashani-Nejad, S., Dalvi, A. D., Voermann N., Candy, I. M. and Wasmund, B. 2009. Future of rotary kiln – electric furnace (RKEF) processing of nickel laterites, in Proc. European Metallurgical Congress 2009, (ed. J. Harre), 943-974, GDMB-Informationsges, Clausthal-Zellerfeld.

Warner, A. E. M., Diaz, C. M. and Dalvi, A. D. 2006. World nonferrous smelter survey, Part III: laterite", *Journal of Metals*, **58**, 11-20.